PARTIAL ADMISSION VS. SLIDING PRESSURE APPLIED TO DSG SOLAR PLANT BASED ON LINEAR FRESNEL REFLECTOR

M. Binotti, A. Giostri, M. Astolfi, L. Colombo, E. Macchi, G. Manzolini*

*corresponding author: Ph: +39 02 2399 3810, E-Mail: giampaolo.manzolini@polimi.it

Abstract

Parabolic trough collectors can be considered the reference technology for large scale Concentrating Solar Power plants (CSP). A significant cost reduction is expected using solar field based on Linear Fresnel Reflectors (LFR) or, alternatively, compact Linear Fresnel Reflectors (CLFR) characterized by cheaper mirrors and structures. These technologies are here investigated focusing on control strategy optimization when direct steam generation (DSG) in solar field is applied. Technical data and performances of commercial Fresnel plant are considered in this work. Both optical and thermal analysis of the solar field are performed, and the obtained results are used as input for the commercial code Thermoflex 21 which predicts performances of the entire plant. At design conditions, the highest overall efficiency is performed when sliding pressure control is applied achieving a net electric efficiency of 19.25%. Focusing on yearly performances, at current turbine performances, there is no significant difference between sliding pressure or partial admission control strategy: both achieve a sun to electric efficiency of about 10%.

Keywords: Fresnel, Ray-tracing, thermal analysis, Partial Admission, Sliding Pressure, DSG

1 Introduction

Among renewable technologies, a wide diffusion of solar thermal plants is foreseen in the near future mainly because of their capability of decoupling solar energy from electricity production thanks to thermal storage. The main issue that currently limits their diffusion is the high investment costs, and the limited equivalent operating hours (about 3000 hrs vs. 7500 hrs of fossil fuelled power plants). For this reason, research has focused on innovative system aiming at cost reduction. Fresnel is considered a promising technology thanks to ground based mirrors that limit land occupation and reduce wind drag effect allowing the adoption of lighter structures with possible economic advantages. Another potential advantage derived by ground mirror position can be the easier cleaning with benefits for their average reflectivity.

This technology is here investigated focusing on control strategy optimization when direct steam generation (DSG) in the solar field is applied. Technical data of commercial Fresnel plant are considered in this work and used as input for optical and thermal analysis of the solar field: a ray tracing in-house model was developed to predict optical performances of Fresnel collectors, and a spatial discretization approach was used to determine collector thermal losses.

The commercial code Thermoflex 21 [1] was used to predict performances of the entire solar plant. The target of this work was to determine the best operating strategy for a Fresnel collector with Direct Steam Generation. In off-design conditions, two different operation strategies can be adopted: constant pressure at turbine admission and sliding pressure. In the first case solar field outlet pressure is constant and equal to the nominal conditions (55 bar). In the second case, solar field steam pressure decreases together with the steam mass flow generated.

All the investigated plants had similar boundary conditions as well as power block layout and solar field area in order to stress advantages and drawbacks of each control strategy. A wet cooling tower was considered for heat rejection and no heat storage was implemented.

2 Optical analysis

Optical analysis of the Fresnel collector was performed with a built-in ray-tracing model implemented in Matlab®. The model can predict optical performances of different Fresnel collectors, the efficiency decay with transversal and longitudinal incidence angle (IAM curves), and the heat flux distribution on the absorber tube. The code was tested with the collector NOVA 1 by NOVATEC SOLAR starting from the features reported in [2]. However, further assumptions were made in order to completely define the geometry and the optical characteristics of the collector. Three different curvatures for internal, medium and external primary mirrors were selected in order to match IAM curves available in the Thermoflex database which have been provided by NOVATEC SOLAR. Transmittance and absorbance variation with incidence angle for the cover glass and absorber tube was assumed according to [3]. Main geometric and optical characteristics assumed for the simulated absorber are summarized in Table 1.

Assumed characteristics for NOVA 1 collector	
Number of primary mirrors	16
Curvatures [m]	17/20/24
primary mirrors reflectivity	0.92
Secondary mirrors reflectivity	0.95
Cover glass maximum transmittance([1])	0.95
Absorber tube maximum absorbance ([2])	0.94
CPC aperture [m]	0.30
CPC acceptance angle [°]	56
Absorber outer diameter [m]	0.07
σ_{SUN} [mrad]	2.8
$\sigma_{PRIMARY\ MIRROR}$ [mrad]	5

Table 1 - Geometrical and optical properties assumed for NOVA 1 collector simulation

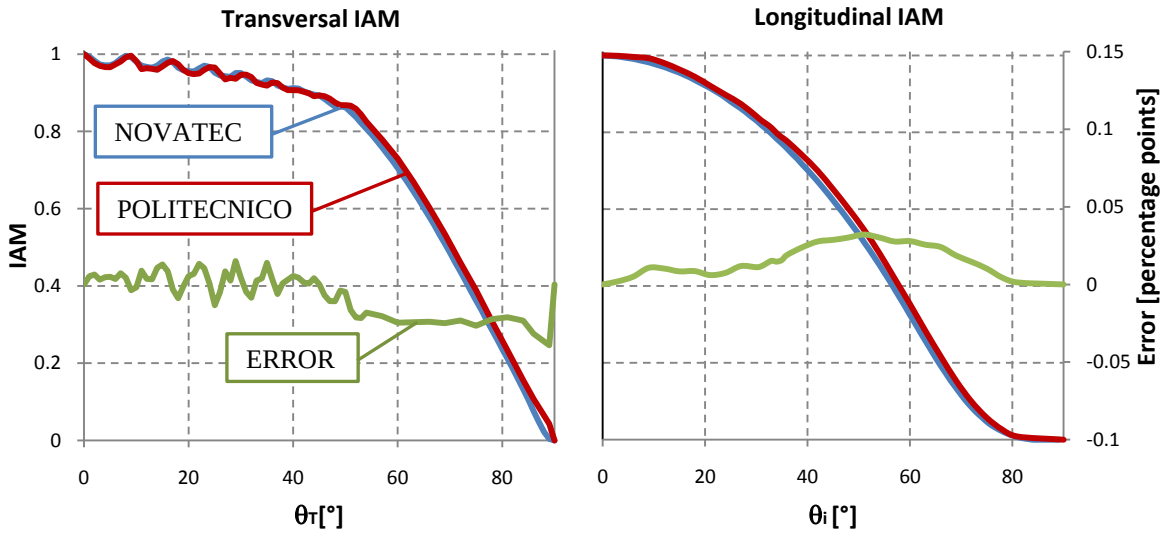

Figure 1 - Longitudinal and transversal Incidence Angle Modifier (IAM) trend as a function of incidence angle

[1] $A_{\mathrm{ABSORBER}} = 6.042 \cdot 10^{-11}\varphi^6 - 1.393 \cdot 10^{-8}\varphi^5 + 1.122 \cdot 10^{-6}\varphi^4 - 3.985 \cdot 10^{-5}\varphi^3 + 6.142.10^{-4}\varphi^2 - 0.0031746\varphi + 0.94$

[2] $\tau_{COVER\ GLASS\_} = -6.826 \cdot 10^{-8} * \varphi^4 + 6.3 \cdot 10^{-6}\varphi^3 - 0.0002\varphi^2 + 0.00183\varphi + 0.95$

The calculated transversal and longitudinal IAM curves are presented in Figure 1 together with the reference NOVA 1 showing good agreement (a maximum error of 0.04%points at angles higher than 50° can be noted). The oscillating trend of the transversal IAM for θ_T between 0° and 50° is due to the passage of the secondary receiver shadow on reflecting mirrors. One mirror out of sixteen is partly shadowed, leading to a limited impact on the resulting curve.

Figure 2 shows a detail of the absorber tube and the graphic output of the ray-tracing program. The resulting heat flux distribution on the absorber tube, also presented in Figure 2, is consistent with similar studies carried out for NOVA 1 collector [4]. It must be outlined that resulting heat flux depends on several assumptions some of which are not referenced (e.g. primary mirror curvature). These may lead to errors in predicted performances and fluxes.

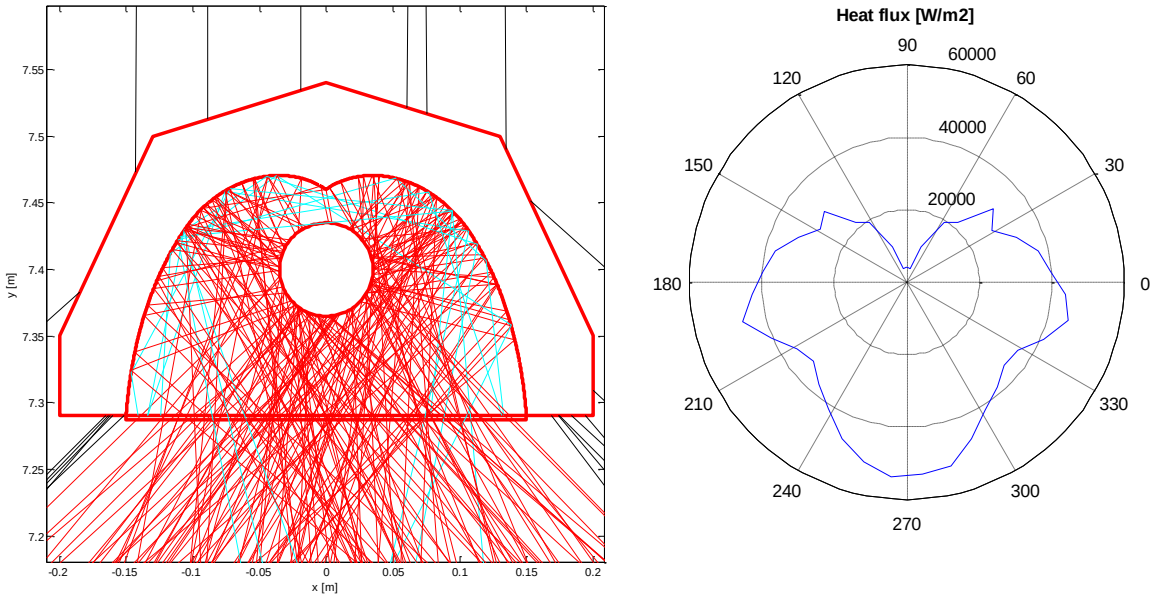

Figure 2 - Ray-tracing screenshot of the secondary reflector and map flux on the absorber tube (DNI=900 W/m^2, $\theta_I = \theta_T = 0°$)

3 Thermal analysis

The thermal analysis was performed in 2D with a finite element software. The conjugate heat transfer problem (conduction in solid structures, free convection and radiation) within the cavity, was solved. Free convection was treated by the incompressible ideal gas model. Because of the intrinsically unstable phenomenon, a transient solver was used to model the problem. The simulation was considered completed when pseudo-stationary condition was reached (maximum temperature variations below 0.1°C).

The absorber tube is made of coated steel guaranteeing low emissivity and is placed in an air gap encapsulated with a cover borosilicate glass that protects the absorber tube from sand and wind as well as reduces heat losses. The back of the secondary reflector is insulated with glass fiber blanket that limits thermal losses from the upper part of the collector. Thermal properties of the components, i.e. thermal conductivity, density and specific heat, were taken from the material library available in the software, while the infrared emissivities for all the surfaces were assumed according to Table 2. The collector heat losses were simulated investigating the absorber surface temperature between 180°C and 300°C, covering the typical operating conditions range.

In order to validate the 2-D model for the thermal analysis, the experimental measurement was reproduced for NOVA-1 solar collector. Differently from real operating conditions, solar collectors thermal losses are

usually calculated heating up the tube with an electric resistance [5], and then measuring the power required to keep the absorber tube at constant temperature without considering solar radiation.

Absorber tube emissivity	0.1-0.12
Cover glass emissivity	0.86
Secondary reflector emissivity	0.2
External cover emissivity	0.5
Ambient convective cooling coefficient [W/m^2-K]	10
Ambient temperature [°C]	40

Table 2 - Parameters for the thermal simulation

Thermal losses calculated with the 2D finite element software were about 33% and 37% lower than NOVA-1 values in the Thermoflex library (see Figure 3) for an absorber emissivity of 0.12 and 0.10, respectively. This difference can occur because of uncertainties on real collector thermal properties, in particular the absorber emissivity, and because of the 2D approximation: actually, due to the relevant tube length, instabilities of the plume might arise in the longitudinal direction causing the formation of thermals. Furthermore, this perturbation could make the flow turbulent. The combination of these effects could significantly enhance the heat transfer.

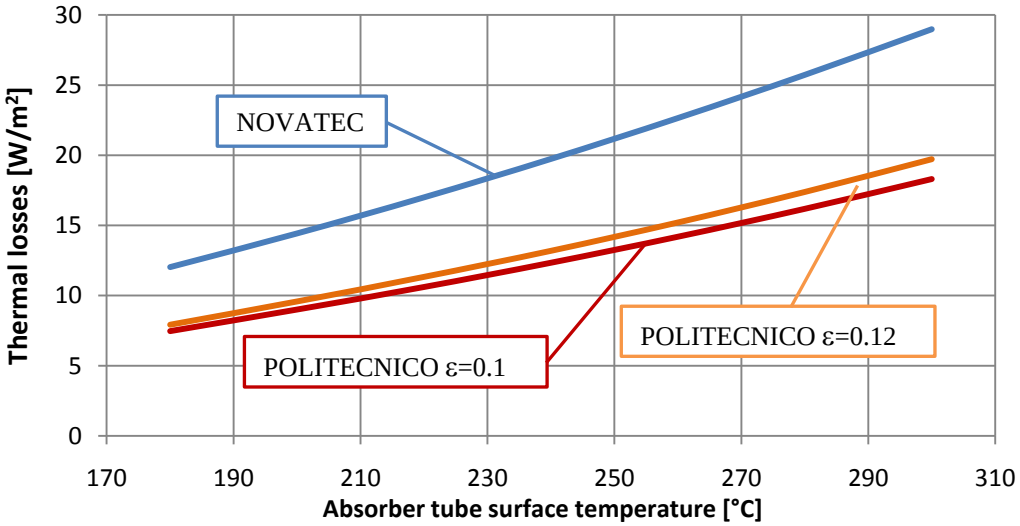

Figure 3 - Thermal losses of the NOVA 1 type collector per square meter of primary reflector

Finally, a simulation of real operating conditions with heat fluxes on the collector calculated with the ray-tracing model abovementioned was performed. The following input were considered: i) flux on the absorber tube, ii) flux absorbed by the secondary reflector, iii) flux absorbed by the cover glass (solar radiation not transmitted nor reflected by the mirror). The simulation was carried out assuming a constant temperature on the inner side of the tube. In this case, calculated thermal losses ranged from 1W/m^2 at 180°C to 12 W/m^2 at 300°C, thus significantly lower than reference case and previous simulations. This is because the temperature of secondary reflector and the cover glass are higher than experimental conditions, lowering the radiative heat transfer between the absorber tube and the surrounding surfaces. The flow structure and temperature profiles are completely different from the previous case as shown in Figure 4. In particular, it is possible to notice a strong temperature increase where the majority of the sun rays intercept the secondary reflector.

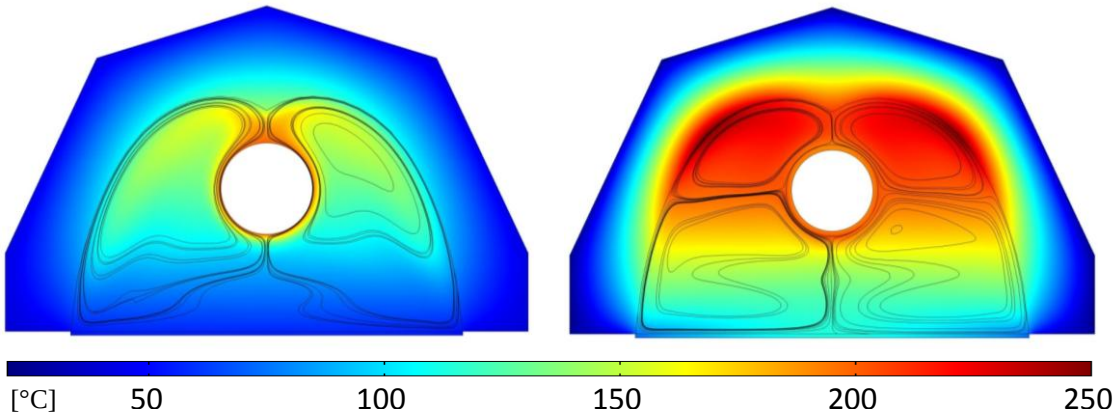

Figure 4 - Temperature contours and velocity streamlines for a collector in experimental (left) and real (right) operating conditions

Considering that it was not possible to validate these results with any experimental measurement, for the yearly simulations of the solar plant, thermal losses available in the Thermoflex library in accordance with NOVATEC SOLAR were used.

4 Solar plant simulation

As aforementioned, the investigated solar plant was based on direct cycle configuration (DSG) in which steam is directly heated in solar field. DSG technology has some advantages against indirect technology (where a heat transfer fluid flows in the solar field) that can be summarized in: (i) constant temperature in the solar field during phase transition with a consequent higher thermal efficiency, (ii) solar field exit temperature equal to the maximum steam cycle temperature, (iii) heat exchangers are no more necessary with investment cost and thermal efficiency advantages, and (iv) reduction of mass flow rate in the solar field reducing field auxiliaries consumption.

4.1 Sizing

The investigated DSG plant was based on a saturated Rankine cycle with steam turbine inlet pressure equal to 55 bar corresponding to a temperature equal to 270°C. Steam quality (x_v) at solar field outlet was set to 0.80 according to real plant available data [6]. The water-steam mixture exiting the solar field is sent to a phase separator from which dry steam is fed to turbine whereas liquid fraction is mixed with pre-heated water coming from preheating line.

Heat rejection was performed via an evaporative cooling tower with a design condensing pressure of 0.08 bar. Dry bulb temperature and relative humidity were assumed equal to 35 °C and 17% respectively.

A schematic of DSG solar plant is shown in Figure 5.

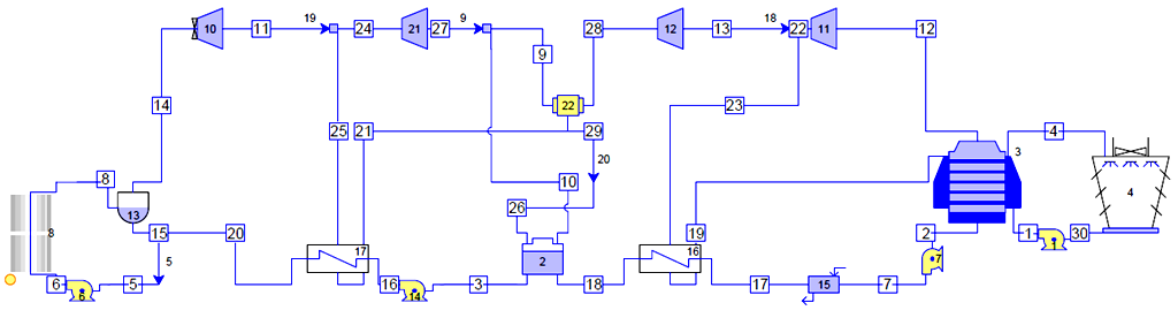

Figure 5 - Fresnel plant layout (Screenshot from Thermoflex® 21)

Performances of plant components were modeled with Thermoflex® built-in correlations. In particular, steam turbine sizing was performed adopting ST-Assembly feature which has an accurate prediction of stage isentropic efficiency and last stage exhaust losses.
Three different steam turbine control strategies were analyzed: (i) throttle control ("THR") with a valve at turbine inlet which keeps the target pressure, (ii) sliding pressure control ("SL" and "SL90") that allows pressure to float according to load, and (iii) partial admission ("PAR") where a control valve control steam flow in nozzles. Depending on the adopted control strategy, Thermoflex suggests different isentropic efficiency for the first steam turbine group. In SL90, an advanced turbine design with very high efficiency was set.

4.2 Performance at design conditions

In Table 3, main solar plant characteristics and performance are summarized using efficiency indexes already discussed in [7]. In order to make a consistent comparison among the different investigated control strategies, solar field was kept constant for all studied cases, thus the gross power at on-design condition varies, because of first stage turbine efficiency assumption (see **Error! Reference source not found.**).

SOLAR FIELD				
Total SCA aperture area [m^2]	288,610			
Number of operating flow paths	43			
Solar Field ΔP [bar]	10.89			
Solar field aux cons. [MW][3]	0.20			
$\eta_{optical}$ [%]	63.65			
$\eta_{thermal}$ [%]	95.40			
η_{piping} [%]	99.78			
POWER PLANT				
	SL	SL90	THR	PAR
Gross power [MW]	52.40	53.32	52.29	52.10
Net power [MW]	50.00	50.90	49.87	49.68
Cooling tower aux cons. [MW]	0.82	0.82	0.82	0.82
η_{net_PB} [%]	31.90	32.45	31.81	31.69
η_{aux_SF} [%]	99.60	99.60	99.60	99.60
$\eta_{overall}$ [%]	19.25	19.59	19.20	19.13

Table 3 - Performance of solar field and power plant

Adoption of sliding pressure control has limited advantages at design conditions (less than 1%); advantages increases if an advanced design of the first stage is assumed. From this results, it seems that sliding pressure control is the best strategy for Fresnel solar plant with DSG .

4.3 Off-Design simulation

In Figure 6, the net solar field efficiency and gross power block efficiency are displayed as a function of DNI and control strategy. Solar field efficiency is defined as the ratio between net thermal power delivered by the collector field and the available solar power, while power block efficiency as the ratio between net power output and thermal input at the power cycle.

[3] Power of recirculating pump of solar field

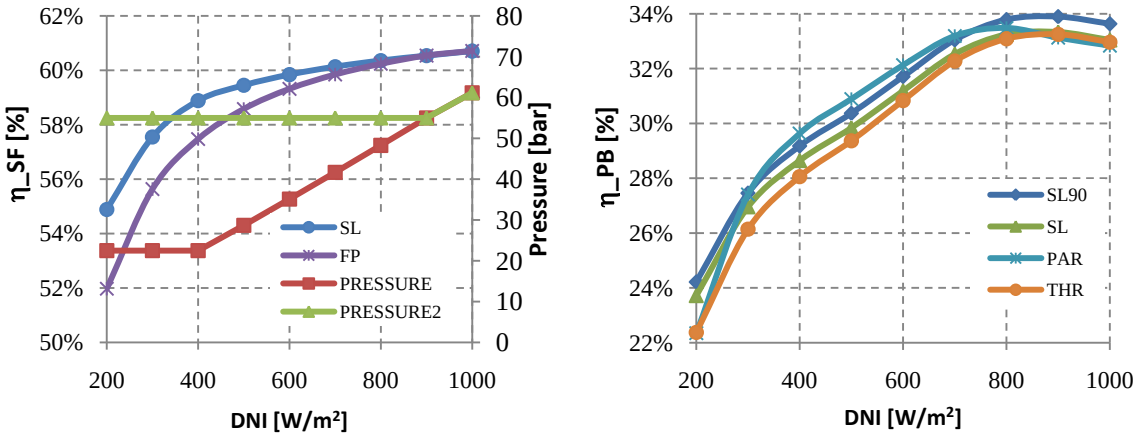

Figure 6 - Net solar field efficiency (left) and power block gross efficiency (right) as function of DNI (T_{WB}=17.9 °C)

The different control strategies considered in this work have an impact both on power section efficiency and on solar collector behavior: SL has higher solar field efficiency than PAR and THR cases because of lower evaporation pressure and temperature at partial load which reduces solar field thermal losses. For PAR and THR cases, collector temperature is equal to design conditions. It can be noted that at DNI higher than design conditions, pressure at turbine inlet increases for all cases; collectors must be designed to support pressure condition at highest DNI.

Focusing on power block gross efficiency, partial admission has the highest efficiency between 300 and 700 W/m^2. This is because it takes advantage of an higher pressure ratio, with only minor reduction of turbine efficiency in the first stages. However, PAR is penalized at very high and very low radiation, while THR achieves the lowest efficiency in all conditions. SL and SL90 have similar trend just shifted.

5 Yearly Results

Yearly simulations were performed using Thermoflex 21® with one hour time step dependent on available weather data. In this work, Las Vegas (USA) was selected as location of the plant and weather data, necessary to predict yearly energy performances, were taken from TMY3 database [8].

Results for all the studied cases are summarized in Table 4. Available solar energy represents the total amount of energy that would be collected by the solar field (DNI multiplied by solar total collector aperture area[4]). Receiver solar energy takes into account optical losses and represents the solar energy impinging on absorber tube.

	SL	SL90	THR	PAR
Available solar energy [MWh/y]	748063	748063	748063	748063
Receiver solar energy [MWh/y]	289937	289937	289829	289833
Net electric energy [MWh/y]	74594	75986	72409	74524
$\eta_{optical}$ (%)	38.76	38.76	38.74	38.74
$\eta_{thermal}$ (%)	93.30	93.31	92.05	92.06
η_{piping} (%)	99.76	99.76	99.75	99.75
η_{net_PB} (%)	27.81	28.33	27.37	28.16
η_{aux_SF} (%)	99.39	99.40	99.42	99.43
$\eta_{overall}$ (%)	9.97	10.16	9.68	9.96

Table 4 Yearly results for investigated cases

[4] Total collectors aperture area is the sum of all reflective areas of primary mirrors

About optical efficiency, the minimum difference among four investigated cases is not because the control strategy affect it, but because the different power block efficiency leads to different DNI limit at which power plant shut down occurs: SL works 3 hours more than PAR case. About thermal efficiency, the advantage of sliding pressure control can be quantified in 1.3% point. From yearly average power block, besides SL90, PAR achieves the highest value because solar plant works between 500 and 800 W m^{-2} for most of the year.

Focusing on overall performance, also named sun-to-electric efficiency, it is in the range of 10% for all cases. There is no significant difference between sliding pressure and partial admission, with current first stage design, while SL is better with improved efficiency. Second consideration is that throttling leads to worst efficiency performances. Finally, it must be reminded that performance calculations were run assuming NOVA 1 thermal losses implemented in Thermoflex, which are greater than those predicted by the 2-D finite element software.

6 Conclusions

This work presented an analysis to optimize performances of a solar plant based on Fresnel collector and with Direct Steam Generation. Three different tools were adopted: one to determine optical efficiency and flux distribution on the collector, the second to calculate collector thermal losses and, finally, Thermoflex to assess overall plant performances. Calculated thermal losses at typical operating conditions were significantly lower than available data in literature. Because results couldn't be validated, referenced values were assumed, however further studies has been going on to justify these discrepancies.

As far as optimal operating strategy is concerned, at current turbine performances, no significant difference can be noted between partial admission and sliding pressure; both achieves a overall yearly efficiency of about 10%. Future work will focus on thermal analysis as well as different secondary reflector to improve Fresnel performances

References

1. **Thermoflow.** *Thermoflex Help System.* 2011.
2. **Novatech Biosol.** Technical data - NOVA 1. 2009.
3. **Mertins, M.** Technische und wirtschaftliche Analyse von horizontalen Fresnel-Kollektoren. 2009.
4. **M. Selig, M. Mertins.** From saturated to superheated direct solar steam generation - technical challenges and economical benefits. *Proceedings of SolarPACES 2010.* 2010.
5. **Burkholder, F. and Kutscher, C.** *Heat Loss Testing of Schott's 2008 PTR70 Parabolic Trough Receiver.* s.l. : NREL - Technical Report NREL/TP-550-45633, May 2009.
6. **Zarza, E., et al.** INDITEP: The first pre-commercial DSG solar power plant. *Solar Energy.* Elsevier, October 2006, Vol. 80, pp. 1270-1276.
7. **A.Giostri, M.Binotti, P.Silva, E.Macchi, G.Manzolini.** Comparison of two linear collectors in solar thermal plants: parabolic trough vs Fresnel. 07-10 August 2011, Washington (US).
8. National Solar Radiation Data Base. [Online] http://rredc.nrel.gov/solar/old_data/nsrdb/1991-2005/tmy3/.